Proton Transfer of Excited 7-Azaindole in Reverse-Micellar Methanol Nanopools: Even Faster than in Bulk Methanol

Oh-Hoon Kwon and Du-Jeon Jang*

School of Chemistry, Seoul National University, NS60, Seoul 151-742, Korea

Received: February 11, 2005

The methanol-catalyzed double-proton transfer of photoexcited 7-azaindole in the free cores of solvation-restricted reverse micelles takes place on the time scale of 90 ps, even shorter than in bulk methanol. This anomalous rate increase with a large kinetic isotope effect of 5 experimentally proves the widely discussed two-step model for the overall reaction of solvent-mediated proton transfer. On the other hand, the molecules in the bound layers and in the headgroup layers relax in 900 and 6000 ps, respectively, without going through proton transfer. The tautomerization and the relaxation of excited 7-azaindole can be exploited to probe the nanopools of methanol reverse micelles.

Introduction

Proton transfer has been attracting considerable attention because it plays a key role in a wide variety of biological and chemical phenomena. Tautomerization involving H bonds is an example of proton-transfer processes in biological systems.[1−4] The proton-translocating tautomerization of DNA base pairs has been suggested to cause inappropriate pairing of bases to result in point mutations since the discovery of the double helix structure of DNA by Watson and Crick in 1953. Thus, photoinduced proton-transfer reactions are often considered to be useful for understanding the causes of mutagenesis in DNA replications. In this regard, the dimers of 7-azaindole (7AI) molecules are studied prototypically because they are structurally similar to H-bonded DNA base pairs.[1] Alternatively, 7AI is a chromophoric moiety of 7-azatryptophan, a noninvasive in situ optical probe for the structures and dynamics of proteins.[5] A number of researches have been carried out to elucidate the photophysics of 7AI in clusters and solvents such as hydrocarbons, water, and alcohols.[6−19]

The mechanism of the solvent involvement in the tautomerization of 7AI in water and alcohols has been emphasized to possess considerable attraction.[10−19] In particular, the two-step model, such as the scheme involving methanol described in Figure 1, has been widely discussed.[15−19] The first step is solvent reorganization (k_1), that is, formation of a cyclically H-bonded 1:1 7AI·(protic solvent) complex, and the second step is intrinsic proton transfer (k_{pt}) relayed by the complexed solvent molecule. In one limit, solvent reorganization can be the rate-limiting step so that the observed rate constant (k_{PT}) becomes k_1, as reported for 7-hydroxyquinoline embedded in solid polymeric matrixes.[20] In the opposite limit when equilibrium (k_1/k_{-1}) between solvent reorganization and solvent randomization (k_{-1}) is rapid relative to k_{pt}, k_{PT} is independent of solvent dynamics and is expressed as $(k_1/k_{-1})k_{pt}$. The static role of solvation is also reported in the manner of the transition-state theory that $k_{PT} = k_{pt} \exp(-\Delta G^{\ddagger}/k_B T)$. $\Delta G^{\ddagger}$ is the change of free energy for the formation of a cyclically bridged 1:1 complex from the predominant unbridged form.[14] It has been suggested that solvation toward an appropriate configuration is required prior to efficient proton tunneling.[6,14−19]

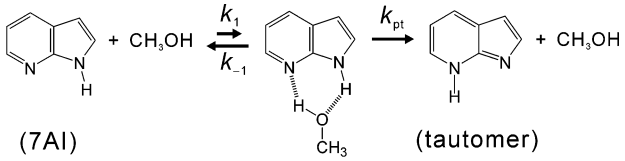

Figure 1. Two-step model for the methanol-catalyzed double-proton transfer of 7AI.

Reverse micelles are interesting systems because they can serve not only as nanoreactors but also as simple biological models. Reverse micelles in hydrocarbon solvents formed by surfactant molecules with their polar headgroups pointing inward can be good candidates for the exploration systems of biological membranes, water molecules confined in biologically relevant surroundings, and solvation dynamics.[21−23] Although aqueous reverse micelles have been intensively studied, considerably less efforts have been made on studying nonaqueous reverse micelles. Reverse micelles have been investigated using the surfactant of Aerosol-OT (AOT, sodium dioctylsulfosuccinate) to partition nonaqueous polar solvents of methanol, acetonitrile, ethylene glycol, propanediol, formamides, and urea in hydrocarbon solvents.[24−33] Also explored were intramolecular charge transfer,[25−27] solvation,[25−29] and alkaline hydrolysis[30] in nonaqueous reverse micelles. However, proton transfer has not been studied in nonaqueous reverse micelles yet to our knowledge. We note that the luminescence properties of 7AI in aqueous reverse micelles have been reported without showing any evidence of proton transfer.[34]

In these regards, we were tempted to investigate the proton-transfer processes of 7AI in the nanopools of methanol confined in AOT reverse micelles. Our results obtained using time-resolved fluorescence spectroscopy show the solvent-assisted tautomerization of 7AI in the methanol nanopools of AOT reverse micelles for the first time to our knowledge. The perturbation of solvent equilibration in methanol nanopools accelerates proton transfer, proving the two-step model. We also show that proton transfer and relaxation can be utilized to probe the dynamic and energetic properties of methanol nanopools confined within micelles.

Experimental Section

7AI (99%), *n*-heptane (anhydrous), CH_3O^1H (anhydrous), and CH_3O^2H (isotopic purity ≥ 99.5%) were used as purchased from

* Corresponding author. E-mail: djjang@snu.ac.kr.

10.1021/jp050743c CCC: $30.25
Published on Web 03/22/2005

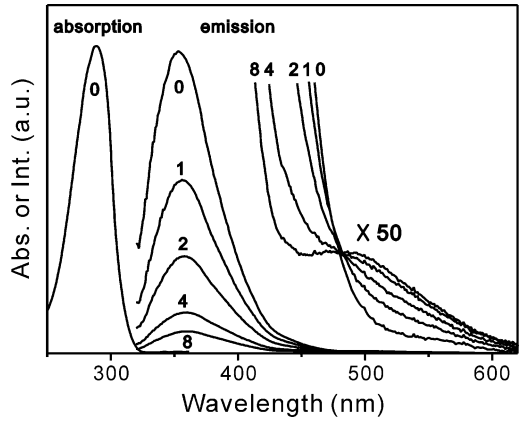

Figure 2. Absorption and emission ($\lambda_{ex} = 290$ nm) spectra of 7AI in methanol reverse micelles having indicated values of $R_{OH/s}$.

Sigma-Aldrich. AOT (>99%, Sigma-Aldrich) was dried over molecular sieves (4 Å, Merck). 7AI-dissolved AOT micelles, having 0.05 7AI molecule per micelle in average, were prepared by adding 2×10^{-5} mol of 7AI to a 100-mL solution of 0.09-M AOT in *n*-heptane. The employed concentration of 7AI is not expected to change structural properties of AOT micelles. The molar ratio of methanol to AOT ($R_{OH/s}$) was adjusted by adding methanol several hours later. Samples were transparent and monodisperse.

Absorption and emission spectra were obtained by using a UV−vis spectrometer (Scinco, S-2040) and a fluorimeter consisting of a 75-W Xe lamp (Acton Research, XS432) and a 0.30-m monochromator (Acton Research, Spectrapro-300), respectively. Fluorescence kinetic profiles, excited by 25-ps pulses of 288 nm from a Raman shifter pumped with 266-nm pulses from a mode-locked Nd:YAG laser (Quantel, YG701), were detected with a 10-ps streak camera (Hamamatsu, C2830). Fluorescence kinetic constants were extracted by fitting profiles measured at room temperature to computer-simulated exponential curves convoluted with instrumental response functions (fwhm: 40 ps).

Our spectroscopic and kinetic results indicate that practically all of the molecules of 7AI exist within AOT micelles. Because methanol in solutions of AOT and nonpolar solvents is suspected to be slightly present outside reverse micelles,[24] we have checked whether 7AI also exists out of reverse micelles or not. In neat *n*-heptane, the normal fluorescence of 7AI decays on the time scale of 1600 ps, while the emission of tautomers, presumably generated from 7AI dimers, decays in 3600 ps. In (1% in v) CH_3O^1H (CH_3O^2H)-added *n*-heptane, 7AI, presumably 1:1 complexed with methanol, undergoes proton transfer to produce tautomers having a lifetime of 1200 (1700) ps. None of the lifetimes mentioned above have been observed in our AOT-added *n*-heptane samples. Thus, we are confident that practically all of the 7AI molecules incorporate into the nanopools of reverse micelles.

Results and Discussion

The lowest absorption band of 7AI having the maximum at 289 nm is spectrally insensitive to the addition of methanol into AOT reverse micelles (Figure 2), as it was reported to be insensitive to the polarity of the surrounding medium.[15,34] However, the emission spectrum of 7AI changes drastically with $R_{OH/s}$ variation in both aspects of intensity quenching and bathochromic shift. The intensity maximum of emission from the normal species shifts from 351 to 358 nm as $R_{OH/s}$ changes from 0 to 8. This indicates that the overall polarity of methanol

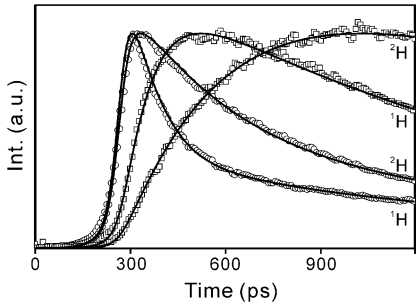

Figure 3. Fluorescence kinetic profiles, monitored at 360 (○) and 550 nm (□), of 7AI in CH_3O^1H (^{1}H) and CH_3O^2H reverse micelles (^{2}H) at $R_{OH/s} = 6$. Lines are best-fitted kinetic curves.

TABLE 1: Fluorescence Kinetic Constants of 7AI in Methanol Reverse Micelles

$R_{OH/s}$	isotope[a]	λ_{em} (nm)	rise time (ps)	decay time (ps)
0		360	instant	6200
1		360	instant	90(11%)[b] + 900(06%) + 6200
		550	94	1400
2		360	instant	90(43%) + 900(22%) + 5900
		550	86	1400
4		360	instant	86(65%) + 900(21%) + 5800
		550	88	1400
6		360	instant	86(73%)[c] + 900(20%) + 5500
		550	88	1400
	^{2}H	360	instant	360(67%)[c] + 1300(20%) + 7200
	^{2}H	550	430	2100
8		360	instant	90(76%) + 900(19%) + 5200
		550	85	1400
∞[d]		360	instant	130
		550	130	690

[a] Protic hydrogen is ^{1}H if not specified otherwise. [b] Initial intensity percentage of each component. [c] All three processes, of course, compete to relax the 7AI molecules in the free cores. The percentage of the fast component for the ^{2}H isotope becomes smaller than that for the ^{1}H isotope because the rate of the fast process becomes remarkably retarded with ^{2}H exchange to get closer to the rate of the medium component. [d] Bulk methanol.

nanopools confined in reverse micelles increases with $R_{OH/s}$ increment, as is a common phenomenon in reverse-micellar systems.[26−28] The magnified visible regions of emission spectra in Figure 2 show that the remarkable decrease of the normal emission with $R_{OH/s}$ increase is accompanied by the concurrent growth of green emission from the tautomeric species.[6,15−17] Considering single emission in methanol-free micelles and dual emission in methanol-added micelles as found in bulk alcohols,[15,16] we infer that the solvent-assisted excited-state proton transfer of 7AI depicted in Figure 1 is operative in the nanoscopic pools of methanol reverse micelles as well.

For 7AI in CH_3O^1H reverse micelles having a $R_{OH/s}$ of 6, the normal emission shows a multiexponential decay profile composed of 86 (73%), 900 (20%), and 5500 ps (7%), while the tautomeric emission rises on the time scale of 88 ps and decays in 1400 ps (Figure 3 and Table 1). The rise time is identical to the fast-decay time of the normal emission within our experimental errors. We have measured steady-state intensities of tautomer emission with variation of $R_{OH/s}$ and normalized them by considering absorbances at the excitation wavelength of 290 nm, the fractions of the fast-decaying components, and tautomer lifetimes to check a possibility that any nonradiative processes other than tautomerization contribute to the fast decay of 7AI in the reverse micelles. Despite substantial overlap between the normal and the tautomer bands, we have found that tautomer fluorescence remains invariant in normalized intensity with

variation of nanopool size within our experimental errors (see Supporting Information). Moog and Maroncelli have already established that the decay of 7AI in bulk methanol is exclusively due to the tautomerization.[16] These designate that the overall rate constant of proton transfer (k_{PT}) for most 7AI molecules in methanol reverse micelles is $(90\ ps)^{-1}$. It is noteworthy that the rate constant observed in solvation-restricted reverse micelles[25−27] is even larger than that of $(130\ ps)^{-1}$ in bulk methanol (Table 1). On the other hand, the other two slower components with no concurrent rise components of the tautomeric emission imply that some fractions of 7AI in methanol reverse micelles relax on the time scales of 900 and 6000 ps without going through tautomerization. The multiphasic decay of the normal emission indicates that 7AI molecules experience distinguishably different three types of environment in methanol reverse micelles having a $R_{OH/s}$ of 6. Furthermore, considerable isotope effects were observed when protic ^1H was substituted by ^2H. The kinetic isotope effect (KIE) of k_{PT} is as large as 4.9, whereas the KIEs of the medium- and the slow-decay components are as small as 1.4 and 1.3, respectively (Figure 3 and Table 1). Of note is that the KIEs of the latter ones are coincidently similar to the KIE (1.5) of the tautomer-relaxation rate. These also suggest that only the molecules showing the fast-decay component undergo proton transfer, whereas the molecules showing the other two components cannot conduce to proton translocation within their relaxation times.

The normal molecules relaxing via the slow-decay process are supposed to reside in the headgroup layers of reverse micelles because the slow-decay time is very similar to the emission lifetime of 7AI in methanol-free reverse micelles. In addition, the wavelength (351 nm) and the lifetime (6200 ps) of 7AI emission at $R_{OH/s} = 0$ are noted to be quite comparable to those (350 nm and 5700 ps, respectively) in a polar aprotic solvent of acetonitrile.[15] The solvent nanopool confined within a reverse micelle can be further divided into the bound layer and the free core according to two-state models.[24−34] The polar solvent molecules located in the core regions of methanol reverse micelles have been suggested to behave like those in bulk solvents, while the molecules trapped in the bound layers are considered to have restricted translational motions.[28,29] Thus, we assign the fast-decay time of 90 ps to the overall proton-transfer time of the 7AI molecules present in free-methanol cores and the medium-decay time of 900 ps to the relaxation time of the molecules in bound-methanol layers. We suggest that 7AI molecules cannot experience proton transfer within their luminescence lifetimes because solvent reorganizational motions are highly suppressed in bound layers. The molecules located in headgroup layers have even longer fluorescence lifetimes than those in bound layers as both translational and rotational motions are almost frozen.

We can distinguish characteristically three different residence sites of 7AI by monitoring kinetically three distinctive types of photoexcited 7AI molecules. The lifetimes of three decay components do not change, but their fractional amplitudes vary with $R_{OH/s}$ variation. With the increase of $R_{OH/s}$, the fast decay component grows at the expense of the slow one (Figure 4 and Table 1). On the other hand, the medium component increases to reach the maximum around $R_{OH/s} = 2$ and then decreases slowly with $R_{OH/s}$. These also support that the 7AI molecules showing the slow and the fast components are present in the headgroup layer and the free-methanol core of a reverse micelle, respectively, while the bound-methanol layer giving the medium component is a spherical shell located between the headgroup layer and the free core. These structures of reverse micelles have

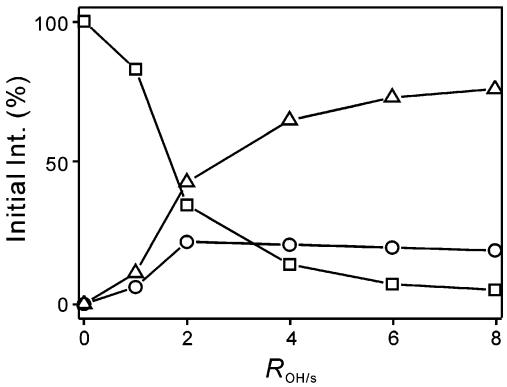

Figure 4. Initial intensity percentages with $R_{OH/s}$ of the fast (△), the medium (○), and the slow (□) decay components for the normal emission of 7AI.

also been proposed with other probe molecular systems by monitoring solvation spectral shift and fluorescence anisotropy.[25−29] Note that the contribution of the fast component grows continuously with $R_{OH/s}$ within our experimental range of $R_{OH/s}$. However, the overall diameter of the methanol reverse micelle measured using dynamic light scattering (3 ± 1 nm at $1.1 \le R_{OH/s} \le 15$) is reported to change hardly with $R_{OH/s}$.[24,28] We then conceive that methanol molecules fill the vacant interior of the reverse micelle gradually with $R_{OH/s}$ to grow the methanol nanopool without expanding the overall size apparently. This differs from the observations that the diameter of an aqueous reverse micelle increases with the molar ratio of water to AOT.[21,22] Thus, we consider that the attractions of methanol molecules to the headgroups of AOT are much weaker than those of water molecules. A few methanol molecules were recently proposed to bridge between a sulfonate headgroup and a cationic counterion in a methanol reverse micelle.[25,26] At low $R_{OH/s}$, methanol molecules are strongly bound to the ionic headgroup layer of the micelle and consequently show slow solvation times.[25−29] As $R_{OH/s}$ increases, overall solvation dynamics in reverse micelles becomes fast because the fraction of the methanol molecules in the bound layer decreases and the fraction in the free core increases. The picture on the structures of methanol reverse micelles based on solvation dynamics is qualitatively consistent with our results. These suggest that the tautomerization and the relaxation of 7AI can be utilized to probe the nanopools of methanol reverse micelles.

We will now discuss the nature of the proton transfer of excited 7AI in methanol reverse micelles and reveal the properties of free-methanol cores, often missed in other reports.[25−28] In aqueous reverse micelles, a subpicosecond solvation process in a free-water core was observed on a time scale similar to that of bulk-water motion.[35] In methanol reverse micelles, the ultrafast solvation process observed in a bulk methanol solution has not been reported due to limited temporal resolutions, although it has been predicted to exist from spectral analysis.[28,29] The proton-transfer time (90 ps) of 7AI in the free cores of methanol reverse micelles remains to be the same within our experimental errors despite $R_{OH/s}$ change (Table 1). It is noteworthy that the k_{PT} of $(90\ ps)^{-1}$ in the free-methanol cores is even larger than that of $(130\ ps)^{-1}$ in bulk methanol despite the observation that the decay time of the tautomer fluorescence is retarded by 2 times in reverse micelles. Also recognized is the prominent KIE of 4.9 in the free-methanol cores, larger than 3.0 in bulk methanol.[16] The formation of cyclically bridged structures is energetically very unfavorable so that 7AI in bulk alcohols exists in a wide range of H-bonded structures.[14,18,19]

Only a small fraction of 7AI molecules in bulk alcohols pose an appropriate H-bonded configuration for facile proton transfer.[14,18,19] Cyclic structures are disfavored in bulk alcohols because of the unfavorable geometry of cyclic H bonds and the expense of networking H bonds involving alcohol molecules.[36−39]

Methanol molecules in the free core of a reverse micelle are considered to be energetically and dynamically different from those in bulk methanol because of the electric field of the micellar charged layer. The properties of water molecules even in the free core region of an aqueous reverse micelle are actually found to be modified from those in bulk water due to the perturbed H-bonding network structure.[32,40,41] The limitation and the strain of H-bond networks raise the energy of methanol in reverse micelles to reduce the free energy of activation ($\Delta G^{\ddagger}$) for the formation of the cyclic complex. Consequently, solvent reorganization, prerequisite to tunnel a proton,[6] becomes energetically less demanding so that the overall proton-transfer rate constant of k_{PT} increases in the free-methanol core. Moreover, the KIE of k_{PT} increases because the solvent-reorganization process contributes less to the overall proton transfer in the nanopool. The cyclic complexes of 1:1 7AI−alcohol in nonpolar solvents having alcohols of low concentrations are recently reported to undergo photoinitiated proton transfer via tunneling with showing KIE of 15 at room temperature.[6] The anomalous behavior of KIE that increases with temperature increment in bulk alcohols has been attributed to the shift of the rate-controlling step from the temperature-dependent and isotope-independent solvation process toward the temperature-independent and isotope-dependent intrinsic proton-transfer event in the overall proton transfer of 7AI.[10,16] The disruption of H-bonding networks of methanol molecules raises the energy of reactants in our systems to reduce $\Delta G^{\ddagger}$ and to lower solvation contribution in k_{PT}. These strongly support the two-step model that the proton-transfer rate of 7AI in bulk protic solvents is determined by the static roles of solvents because of a fast preequilibrium between the unbridged and the bridged normal molecules drawn in Figure 1.[14−19]

In summary, we have shown that the overall proton transfer of excited 7AI in the free-methanol cores of reverse micelles takes place on the time scale of 90 ps with a prominent KIE of 5. The rate constant in the solvation-restricted environment is larger by 50% than in bulk methanol. The disruption of H-bonding networks in reverse micelles reduces the free energy of activation for the formation of 1:1 cyclic complexes. This accelerates the overall proton transfer of 7AI to be faster than that in bulk methanol. The anomalous rate increase with the substantial KIE experimentally proves the widely discussed two-step model for the overall reaction of solvent-mediated tautomerization. On the other hand, the molecules in the bound-methanol layers and in the headgroup layers do not undergo proton transfer within their lifetimes of 900 and 6000 ps, respectively. Thus, we have shown that dynamics for the proton transfer and the relaxation of excited 7AI can be utilized to probe the nanopools of methanol reverse micelles.

Acknowledgment. We are grateful to the Korea Research Foundation for grant KRF-2004-015-C00230. D.-J.J. and O.-H.K. also thank the Strategic National R&D and the Brain Korea 21 Programs, respectively.

Supporting Information Available: Spectroscopic data. This material is available free of charge via the Internet at http://pubs.acs.org.

References and Notes

(1) Douhal, A.; Kim, S. K.; Zewail, A. H. *Nature* **1995**, *378*, 260.
(2) Tanner, C.; Manca, C.; Leutwyler, S. *Science* **2003**, *302*, 1736.
(3) Rini, M.; Magnes, B.-Z.; Pines, E.; Nibbering, E. T. J. *Science* **2003**, *301*, 349.
(4) Osama, K.; Abou-Zied, R. J.; Floyd, E. R. *J. Am. Chem. Soc.* **2001**, *123*, 4613.
(5) Négrerie, M.; Gai, F.; Bellefeuille, S. M.; Petrich, J. W. *J. Phys. Chem.* **1991**, *95*, 8663.
(6) Kwon, O.-H.; Lee, Y.-S.; Park, H. J.; Kim, Y.; Jang, D.-J. *Angew. Chem., Int. Ed.* **2004**, *43*, 5792.
(7) Catalán, J.; del Valle, J. C.; Kasha, M. *Proc. Natl. Acad. Sci. U.S.A.* **1999**, *96*, 8338.
(8) Folmer, D. E.; Wisniewski, E. S.; Hurley, S. M.; Castleman, A. W., Jr. *Proc. Natl. Acad. Sci. U.S.A.* **1999**, *96*, 12980.
(9) Takeuchi, S.; Tahara, T. *Chem. Phys. Lett.* **2001**, *347*, 108.
(10) Konijnenberg, J.; Huizer, A. H.; Varma, C. A. G. O. *J. Chem. Soc., Faraday Trans. 2* **1988**, *84*, 1163.
(11) Catalán, J.; Perez, P.; del Valle, J. C.; de Paz, J. L. G.; Kasha, M. *Proc. Natl. Acad. Sci. U.S.A.* **2002**, *99*, 5793.
(12) Moog, R. S.; Bovino, S. C.; Simon, J. D. *J. Phys. Chem.* **1988**, *92*, 6545.
(13) Smirnov, A. V.; English, D. S.; Rich, R. L.; Lane, J.; Teyton, L.; Schwabacher, A. W.; Luo, S.; Thornburg, R. W.; Petrich, J. W. *J. Phys. Chem. B* **1997**, *101*, 2758.
(14) Mente, S.; Maroncelli, M. *J. Phys. Chem. A* **1998**, *102*, 3860.
(15) Chapman, C. F.; Maroncelli, M. *J. Phys. Chem.* **1992**, *96*, 8430.
(16) Moog, R. S.; Maroncelli, M. *J. Phys. Chem.* **1991**, *95*, 10359.
(17) Chou, P.-T.; Yu, W.-S.; Wei, C.-Y.; Cheng, Y.-M.; Yang, C.-Y. *J. Am. Chem. Soc.* **2001**, *123*, 3599.
(18) Waluk, J. *Acc. Chem. Res.* **2003**, *36*, 832.
(19) Kyrychenko, A.; Stepanenko, Y.; Waluk, J. *J. Phys. Chem. A* **2000**, *104*, 9542.
(20) Kwon, O.-H.; Doo, H.; Lee, Y.-S.; Jang, D.-J. *ChemPhysChem* **2003**, *4*, 1079.
(21) Bhattacharyya, K. *Acc. Chem. Res.* **2003**, *36*, 95.
(22) Nandi, N.; Bhattacharyya, K.; Bagchi, B. *Chem. Rev.* **2000**, *100*, 2013.
(23) Cohen, B.; Huppert, D.; Solntsev, K. M.; Tsfadia, Y.; Nachliel, E.; Gutman, M. *J. Am. Chem. Soc.* **2002**, *124*, 7539.
(24) Riter, R. E.; Kimmel, J. R.; Undiks, E. P.; Levinger, N. E. *J. Phys. Chem. B* **1997**, *101*, 8292.
(25) Hazra, P.; Chakrabarty, D.; Sarkar, N. *Langmuir* **2002**, *18*, 7872.
(26) Hazra, P.; Sakar, N. *Phys. Chem. Chem. Phys.* **2002**, *4*, 1040.
(27) Hazra, P.; Chakrabarty, D.; Chakraborty, A.; Sarkar, N. *J. Photochem. Photobiol., A: Chem.* **2004**, *167*, 23.
(28) Shirota, H.; Horie, K. *J. Phys. Chem. B* **1999**, *103*, 1437.
(29) Hazra, P.; Chakrabarty, D.; Sarkar, N. *Chem. Phys. Lett.* **2003**, *371*, 553.
(30) Mukherjee, L.; Mitra, N.; Bhattacharyya, P. K.; Moulik, S. P. *Langmuir* **1995**, *11*, 2866.
(31) Caponetti, E.; Chillura-Martino, D.; Ferrante, F.; Pedone, L.; Ruggirello, A.; Liveri, V. T. *Langmuir* **2003**, *19*, 4913.
(32) Venables, D. S.; Huang, K.; Schmuttenmaer, C. A. *J. Phys. Chem. B* **2001**, *105*, 9132.
(33) Riter, R. E.; Undiks, E. P.; Kimmel, J. R.; Levinger, N. E. *J. Phys. Chem. B* **1998**, *102*, 7931.
(34) Ray, J. G.; Sengupta, P. K. *Chem. Phys. Lett.* **1994**, *230*, 75.
(35) Riter, R. E.; Willard, D. M.; Levinger, N. E. *J. Phys. Chem. B* **1998**, *102*, 2705.
(36) Asbury, J. B.; Steinel, T.; Fayer, M. D. *J. Phys. Chem. B* **2004**, *108*, 6544.
(37) Matsumoto, M.; Gubbins, K. E. *J. Chem. Phys.* **1990**, *93*, 1981.
(38) Wallen, S. L.; Palmer, B. J.; Garrett, B. C.; Yonker, C. R. *J. Phys. Chem.* **1996**, *100*, 3959.
(39) Haughney, M.; Ferrario, M.; McDonald, I. R. *J. Phys. Chem.* **1987**, *91*, 4934.
(40) Amararene, A.; Gindre, M.; Le Huérou, J.-Y.; Nicot, C.; Urbach, W.; Waks, M. *J. Phys. Chem. B* **1997**, *101*, 10751.
(41) Mittleman, D. M.; Nuss, M. C.; Colvin, V. L. *Chem. Phys. Lett.* **1997**, *275*, 332.